Hindawi
Advances in Materials Science and Engineering
Volume 2019, Article ID 5604197, 8 pages
https://doi.org/10.1155/2019/5604197

Research Article

Rutting and Fatigue Properties of Cellulose Fiber-Added Stone Mastic Asphalt Concrete Mixtures

Muhammad Irfan,[1] **Yasir Ali**,[2] **Sarfraz Ahmed**,[1] **Shahid Iqbal**,[1] **and Hainian Wang**[3]

[1]*Military College of Engineering, National University of Sciences & Technology (NUST), Islamabad 44000, Pakistan*
[2]*National Institute of Transportation, National University of Sciences & Technology (NUST), Islamabad 44000, Pakistan*
[3]*South Erhuan Middle Section, Chang'an University, School of Highway, Xi'an 710064, China*

Correspondence should be addressed to Muhammad Irfan; mirfan@mce.nust.edu.pk

Received 9 August 2018; Accepted 7 March 2019; Published 25 March 2019

Guest Editor: Munir Nazzal

This paper investigates dynamic response, rutting resistance, and fatigue behavior of three stone mastic asphalt (SMA) concrete mixtures selected on basis of nominal maximum aggregate size (NMAS): 25 mm, 19 mm, and 12.5 mm using cellulose fiber added as 0.3% of the total weight of aggregate. Superpave gyratory specimens were fabricated and subjected to the dynamic modulus ($|E^*|$) and flow tests (flow number and flow time) using an asphalt mixture performance tester. The $|E^*|$ test results were employed to develop stress-dependent master curves for each mixture, indicating that the mixture with the NMAS of 25 mm is relatively stiffer than other tested mixtures; this mixture also exhibits excellent strength against rutting failure. In addition, fatigue parameter, which is derived from dynamic response and phase angle, is determined, and results reveal that 12.5 mm NMAS mix has relatively better resistance to fatigue than other selected mixtures. Furthermore, nonlinear regression model specifications were utilized to predict accumulated strains as a function of loading cycles. Also, a flow number model is developed that predicts the rutting behavior of mixtures, and results suggest that model predicted and observed outputs of 25 mm SMA mix are found to be very close. The results of this study help in understanding the performance and behavior of cellulose fiber-added stone mastic asphalt concrete mixtures under varying simulated temperature and stress levels, which can be used in areas where the premature failure of flexible pavements is often observed. The testing protocol employed in this study will also help in evaluating pavement performance using Mechanistic-Empirical Pavement Design Guide.

1. Introduction

Rutting and fatigue in flexible pavements are two of the common distresses manifested on national highways across the globe. Various factors are associated with these distresses including overloading, high temperatures, and empirical design approach used for structural design. To this end, SMA is considered an effective solution in heavily trafficked areas because of larger single size aggregate that can be used with the increased bitumen, thus controlling rutting susceptibility. The resistance to fatigue and reflection cracking is enhanced due to higher binder content in SMA mixtures. In various parts of the world, use of SMA is very common for heavily trafficked areas. The reason for such usage could be the design of SMA mixtures, in which wheel load is endured by the coarse aggregate skeleton that contributes towards resistance to rutting and rich binder that seals the voids and consequently makes it tougher. Thus, the contact among stones in coarse aggregate dominates, whereas the fine and intermediate aggregate sizes assist to grip the coarser particles when the mix is spaced out.

SMA texture characteristically provides good riding quality, better skid resistance along with comparatively little noise. The coarse aggregate provides durability that contributes towards tremendous resistance to permanent deformation, and higher bitumen content seals the voids and makes it exceedingly resilient. The drainage inhibitor is needed to avoid bitumen bleeding throughout the service life

of the pavement structure. To enhance the mechanical properties of SMA, modified bitumen along with suitable additives can be used; and in some situations, it can reduce or even exclude the requirement for other drainage inhibitors.

A considerable improvement has been observed in recent past in relation to the design of the pavement structure where the fundamental mechanistic properties were given substantial importance. Various new pavement mixtures have been developed along with performance-based grading and mixture design/analysis system, more commonly known as Superior Performing Asphalt Pavements (Superpave) by Strategic Highway Research Program (SHRP). Such developments have considerably reduced the industries' reliance on conventional empirical mix design methods, as proposed by Marshall and Hveem across the globe. More discussion is to follow in ensuing sections.

2. Literature Review

Bonaquist et al. [1] recommended three types of performance tests in National Cooperative Highway Research Program (NCHRP) Report 513: dynamic modulus ($|E^*|$), flow number (FN), and flow time (FT) tests for the superpave mix design procedure to predict the performance of designed asphalt mixtures. The $|E^*|$ test was already being used to predict in situ performance of asphalt mixtures, and the use of flow tests (i.e., FN and FT) was very limited. Later, it was more pronounced that the $|E^*|$ test alone is not an accurate predictor of a mix behavior at higher temperatures; more emphasis is now being given to other two performance tests, i.e., FN and FT tests [2]. To shed more light, a detailed literature review is presented below.

Judycki [3] determined the influence of low-temperature physical hardening on stiffness and tensile strength of conventional asphalt concrete and SMA. $|E^*|$ and indirect tensile strength tests were carried out on mixtures after isothermal storage at a temperature of -20°C, at different time intervals up to 16 days. This study concludes that the strength was noticeably increased after storage. Muniandy et al. [4] evaluated the fatigue behavior of modified and unmodified asphalt binder SMA mixtures using a newly developed crack meander technique. The results obtained from the crack analysis test were compared using strain plots obtained from the indirect tensile fatigue test and concluded that fatigue behavior can be determined using the crack appearance method. İskender [5] determined the rutting resistance of basalt and basalt-limestone aggregate combination for SMA using Laboratoire Central des Ponts et Chaussées (LCPC) wheel tracking test. This research study concludes that rutting resistance was decreased with addition of limestone in SMA as fine/filler material. A study illustrates the effects of adding waste polyethylene terephthalate (PET) on stiffness and fatigue properties of SMA mixtures. This research concludes that the stiffness of mixtures increased when a lower amount of PET is added, and PET-reinforced mixtures exhibit higher fatigue lives compared to controlled mixtures (without PET) [6]. Ahmadinia et al. [7] used waste plastic bottles as an additive for SMA mixtures, and 6% by weight of bitumen was found an optimum quantity of PET. This study concludes that introduction of PET into SMA mixtures significantly improves engineering and mechanical properties. Behnood and Ameri [8] utilized steel slag aggregate in SMA, and results indicate that use of steel slag as a surrogate to coarse aggregate enhanced the Marshall stability, resilient modulus, tensile strength, resistance to moisture damage, and resistance to the permanent deformation.

Sengul et al. [9] conducted Marshall Quotient (MQ) approach, repeated creep test (RCT), indirect tensile strength test (ITST), and Laboratoire Central des Ponts et Chaussees (LCPC) Wheel tracking tests on the SBS polymer modified SMA. The results reveal that addition of SBS increased resistance to the plastic deformation and lowered rutting values compared to conventional mixtures. In another study, lime was added to SMA in order to reduce stripping potential and moisture susceptibility. Response surface methodology was used to determine the effect of lime content and grading on stripping potential of SMA using tensile strength ratio (TSR) index and found that lime content of 1% and finest aggregate yielded a TSR optimum value of $91.8\% \pm 0.8\%$ [10]. Cao et al. [11] evaluated $|E^*|$ of SMA (basalt, B-SMA, limestone, L-SMA, and BL-SMA), and results suggest that B-SMA showed better rutting resistance than other tested mixtures. Pasetto and Baldo [12] conducted a comparative analysis of SMAs with electric arc furnace steel slag. The research has been enunciated in a preliminary study of the chemical, leaching, physical, and mechanical properties of the steel slag and concludes that steel slag has satisfied all requirements of road sector technical standards and shows higher mechanical characteristics than other mixtures. Numerous studies indicated the use of the various additives in SMA apart from cellulose fiber [4–6, 9, 11, 13–15]. Different research demonstrated the evaluation of $|E^*|$ and development of master curves [14, 16–28].

The design of the SMA mixture consists of material selection, determining optimum aggregate gradation, selection of additive and its quantity, and optimum binder content. Furthermore, SMA mixtures are supposed to ensure stability and rutting resistance obtained from aggregate contact and interlock; durability of SMA mixtures is obtained by appropriate mixture design including air voids, voids in mineral aggregate, thickness of asphalt film, and filler quantity.

The asphalt concrete material behaves like a viscoelastic material, and its stiffness varies with the temperature. Higher stiffness/modulus in low temperatures (winters) results in fatigue cracking, and lower stiffness/modulus in high temperatures (summers) results in rutting. The strength of the asphalt material is reduced tremendously with higher temperatures as in Pakistan. Hence, it is mandatory to characterize mixtures with an additive using full test protocol of simple performance ($|E^*|$, FN, and FT) for diverse loading and environmental conditions of Pakistan. This study assesses the performance of SMA mixtures having cellulose fiber using three performance tests, i.e., $|E^*|$, FN, and FT. The results obtained from these tests were further

employed to construction master curves and estimation of fatigue cracking by deriving a fatigue parameter.

3. Objective and Scope

The objective of this research is to investigate the performance of various cellulose fiber-added SMA mixtures by varying NMAS. The performance indicators used in this study are $|E^*|$, FN, and FT. The results obtained from $|E^*|$ are used to determine stiffness moduli and to estimate resistance to fatigue cracking based on $|E^*|$ and phase angle values. This study also describes the rutting potential of mixtures using statistical models that use two different nonlinear formulations to express the number of cycles to failure as a function of axial strain. Three different gradations of nominal maximum aggregate size (NMAS) of 25 mm, 19 mm, and 12.5 mm are selected from the gradation bands developed by National Center of Asphalt Technology (NCAT). A 0.3% cellulose fiber by the total weight of the SMA mixtures aggregate was added, and asphalt binder of penetration grade 60/70 was used. Note that different percentages of cellulose fiber were tested during the initial testing phase, and it was found that 0.3% is an optimum quantity that satisfies the Marshall mix design criteria.

4. Methodology

The ensuing sections explain the methodology adopted in this research study and illustrated in Figure 1.

4.1. Selection of Materials. This research study includes testing of three SMA mixtures differentiated by NMAS that are internationally practiced. Three different gradations based on NMAS of 25 mm, 19 mm, and 12.5 mm are selected from the gradation bands developed by National Center of Asphalt Pavements (NCAT) in the National Cooperative Highway Research Program (NCHRP) report [29], and gradations charts for SMA mixtures are presented in Figure 2. The cellulose fibers of 2-3 mm long pressed pellets have been used as an additive to SMA mixtures to enhance film coating on the aggregate, mix stability, and better interlocking of aggregate skeleton. The optimum bitumen content and mix volumetric analysis are presented in Table 1.

Design of SMA mixtures primarily depends on volumetric properties such as air voids, voids in mineral aggregate, voids in coarse aggregate, and binder content. Brown and Haddock [30] presented optimal proportion selection of coarse and fine aggregates. The volume of coarse aggregate is taken as proportion and bulk density of coarse aggregate. Voids in coarse aggregate for 14 mm nominal size aggregate usually range between 41 and 46% for aggregates compacted with binder with no fine aggregate.

Another important consideration in designing SMA is the filler/additive. This study uses cellulose fiber pellets, VIATOP® manufactured by J. Rettenmaier and Söhne, Germany (Figure 3). VIATOP® is pelletized blend of ARBOCEL® ZZ 8/1 (90% by weight) and bitumen 50/70 (10% by weight). Cellulose fibers, as a stabilizing agent, have

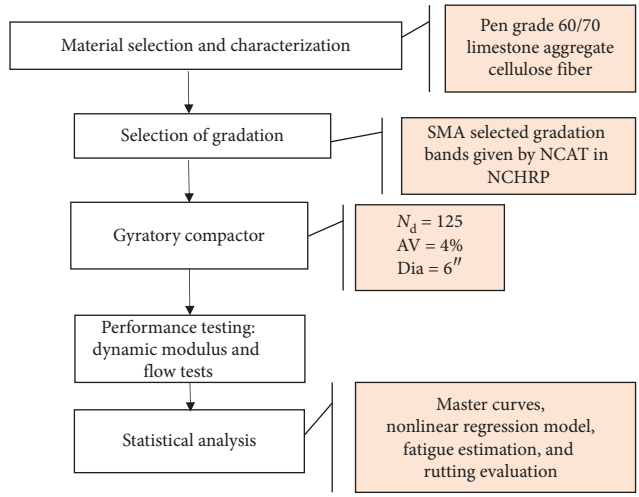

Figure 1: Experimental design of study.

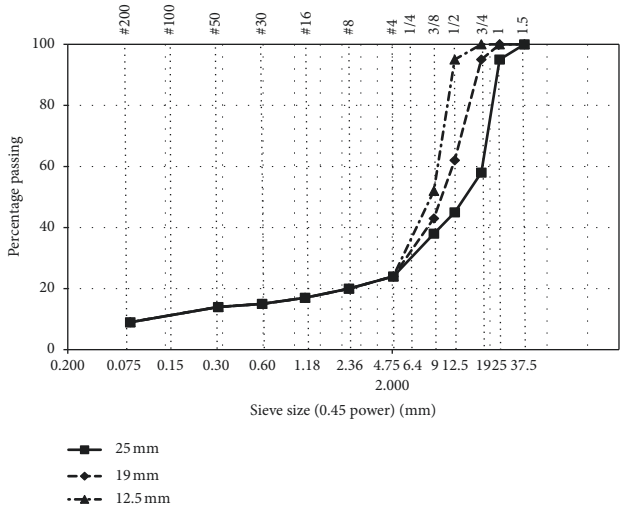

Figure 2: Gradation plot for SMA mixtures.

Table 1: Mix volumetric analysis of SMA mixtures.

Parameters	Mixtures			
	25 mm	19 mm	12.5 mm	Range
Asphalt content (%)	5.30	5.80	6.30	5–7.5
Air voids (%)	5.60	4.90	4.00	4–7
VMA (%)	19.81	18.78	18.01	Min.: 17
VFA (%)	71.73	73.90	78.01	65–80

Figure 3: Cellulose fiber pellets used in SMA mixtures.

a higher asphalt content, thick film coating, high mix stability, improve strength, and less drainage. The optimal quantity of cellulose fiber is based on appropriate quantity of binder and fiber content.

4.1.1. Specimen Preparation. For all performance testing, a superpave gyratory compactor was used to fabricate specimens. The specimens were placed in an oven for short-term aging of 2 hours prior to compaction. The cylindrical specimens with 100 mm diameter were taken from compacted 150 mm diameter gyratory specimens as per the AASHTO standard [31]. The height to diameter ratio of the specimen was kept 1.5 for all tests.

4.2. Performance Testing. Asphalt mixture performance tester (AMPT), which is commonly known as simple performance tester (SPT), is used for $|E^*|$, FN, and FT tests. The equipment has an environmental chamber that manages temperature from 4 to 60°C and confining pressure up to 210 kPa. The $|E^*|$ test is performed at four different temperatures (4.4, 21.1, 37.8, and 54.4°C) and six frequencies (0.1–25 Hz). After completion of the test, the data are acquired from software and employed for development of stress-dependent master curves and fatigue parameter.

AMPT was also used to conduct FN and FT tests. These tests were carried out at a single effective temperature of 54.4°C and deviator stress of 210 kPa. In case of the FN test, the prepared specimens were subjected to a repeated axial haversine compressive loading pulse of 0.1 seconds followed by a rest period of 0.9 seconds. However, for the FT test, the preconditioned specimens were subjected to a constant axial load until it fails, and permanent deformation was measured with respect to the loading time. This test was set to be terminated at 10,000 cycles or until maximum accumulated permanent strain in specimen reached 5%, or whichever came first [32].

5. Results and Discussion

5.1. Dynamic Modulus, $|E^*|$. The $|E^*|$ testing was performed in accordance with AASHTO TP 62-07 [16], which recommends that $|E^*|$ should be evaluated at four different temperatures and six different frequencies in order to develop master curves. The results obtained from the $|E^*|$ test suggest that, for a given loading frequency, an increase in temperature (from 21.1 to 37.8°C), translated into 41, 55, and 26% drop in $|E^*|$ values on average for 25, 19, and 12.5 mm mixtures, respectively. However, for a given temperature and an increase in loading frequency (from 0.1 to 25 Hz), 76, 85, and 74% of the variation in $|E^*|$ values on average were attributed for 25, 19, and 12.5 mm mixtures, respectively.

Since AASHTO TP 62 recommends the development of master curves, it has a few advantages: it allows the comparison of linear viscoelastic materials that are tested at diverse stress rate (loading frequency) and test temperatures, and it can predict $|E^*|$ even at lower temperatures that cannot be obtained from laboratory equipment due to its inability. The average test results are taken for each temperature and used while developing a master curve for average $|E^*|$ at a reference temperature of 21°C using the time-temperature superposition principle, in which each temperature $|E^*|$ value is shifted to a reference temperature to obtain a smooth uniform curve. Microsoft Excel© sheet was used to develop master curves that works on the basis of minimization of error sum of squares to fit the curve. The generic form of the sigmoid function used to construct master curves is given by the following equation:

$$\log\left|E^*\right| = \delta + \frac{\alpha}{1 + e^{\beta+\gamma\left(\log f_r\right)}}, \quad (1)$$

where $\log(|E^*|)$ is the log of dynamic modulus, δ is the minimum modulus value, f_r is the reduced frequency, α is the span of the modulus value, and β and γ are shape parameters.

The maximum stiffness of a mix is a function of the binder at a lower temperature, while at higher temperatures, aggregate interlock overpowers the binder effect and becomes the indicator of mix stiffness. Figure 4 represents master curves for SMA mixtures, which indicated that 25 mm SMA mix has highest $|E^*|$ values at all frequencies while 12.5 mm mixture has lowest $|E^*|$ values.

The $|E^*|$ test values are further employed to derive fatigue parameter that estimates the fatigue resistance of asphalt mixtures [18, 33]. The fatigue parameter is a product of $|E^*|$ and viscoelastic behavior of mix, i.e., phase angle (φ), and can be estimated using equation (2). The fatigue parameter value is inversely proportional to resistance to fatigue cracking. A higher value of the fatigue parameter yields lower resistance to fatigue cracking and vice versa:

$$\text{fatigue parameter} = \left(\left|E^*\right| \times \sin\ \varphi\right), \quad (2)$$

where $|E^*|$ is the dynamic modulus (MPa) and φ is the phase angle (degree). The fatigue parameter evaluates the fatigue resistance of asphalt similar to $|G^* \times \sin\ \delta|$ for asphalt binders. Figure 5 shows the fatigue behavior and resistance to cracking by various SMA gradations, employing the principles of $|E^*|$ and phase angle at a temperature of 21°C. The 25 mm SMA mix shows the highest value for fatigue parameter that translates into minimum resistance to fatigue, whereas the 12.5 mm SMA mix performs relatively better among the tested gradations and exhibits higher resistance to fatigue cracking.

5.2. Flow Tests. The flow number (FN) test was performed in accordance with AASHTO TP 79 [31, 34] and defined as the loading cycle number where tertiary deformation starts. The FN is analogous to field conditions since the loading to the pavement is not continuous. The FN attempts to identify the resistance of a mixture to permanent deformation by measuring the shear deformation that occurs because of haversine loading. The most important output of the FN test is the curve of accumulated strain against the number of loading cycles, which describes the rutting resistance of mixtures (Figure 6). The relationship between the accumulated strain and loading cycles is based on the rutting mechanisms, densification, and shear flow. Figure 6

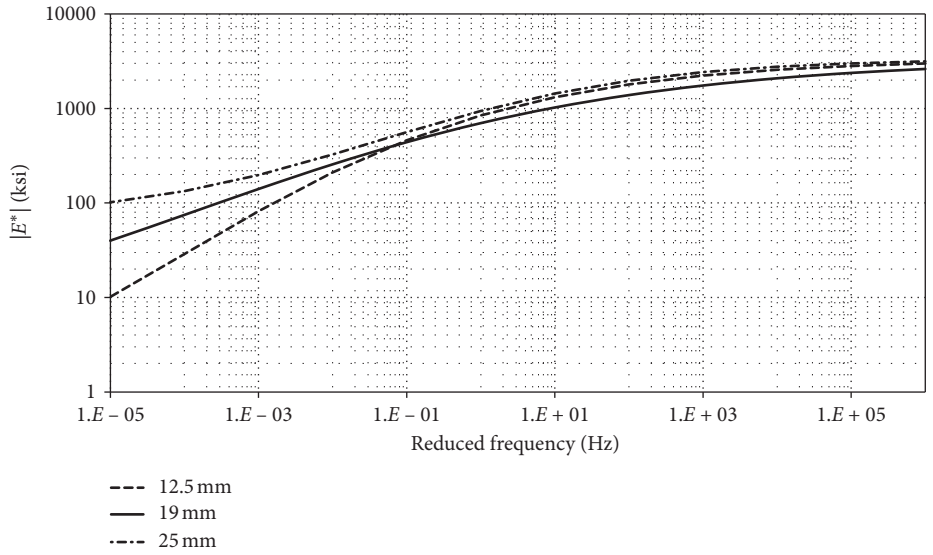

Figure 4: Master curves for SMA mixtures.

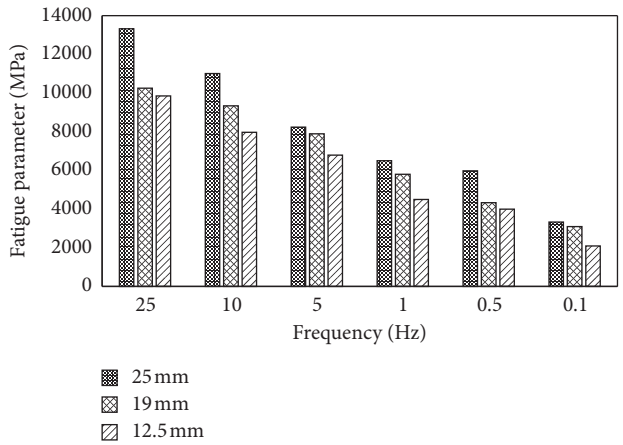

Figure 5: Fatigue parameter of SMA mixtures at 21°C.

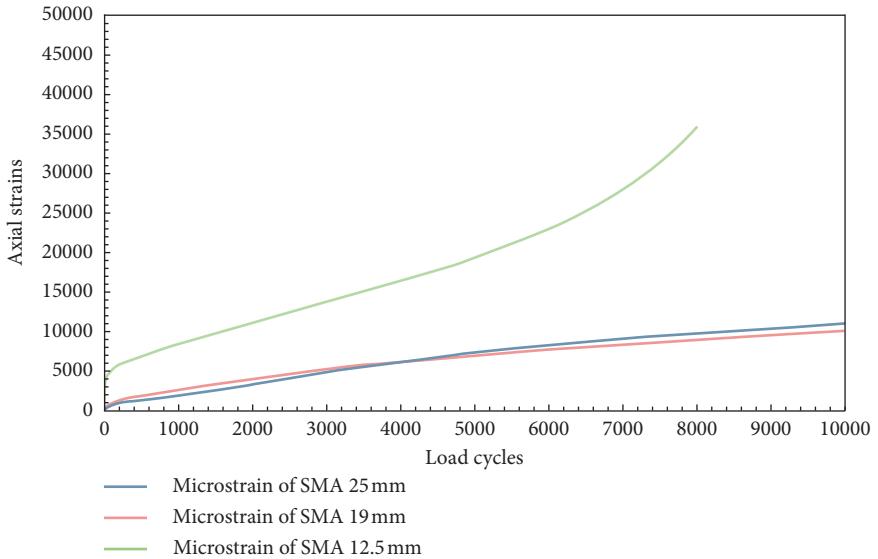

Figure 6: Load cycles versus axial strains.

indicates that only 12.5 mm mix has attained tertiary flow among the tested mixtures. The mixtures do not experience tertiary flow stage; therefore, the number of cycles for the completion of the test is regarded as flow number (FN) of these specimens.

The tertiary flow indicates that the strain rate again increases with loading cycles. When a specimen attains the tertiary stage, the data obtained from AMPT equipment software contain resonance that leads to false FN. In order to remove the noise/resonance from data, data smoothening technique, i.e., five-point moving average, is used to obtain corrected FN (Figure 7). The strain rate, against a designated cycle, is obtained by half of the difference of adjacent cycles. The FN is the start point of the tertiary deformation zone and can be reported as the lowest point in the relationship of rate of change of compliance to loading time. In order to confirm FN value visible as lowest on a curve, the equation is solved by putting y equal to zero as stated by Witczak [31] that theoretically FN is the cycle number corresponding to a rate of change of permanent strain equal to zero. Table 2 illustrates the FN and accumulated strains of SMA, and it is quite clear that 25 mm sustains more loading repetitions than any other tested gradations and less susceptible to rutting. However, other two mixtures experience more strains in short interval of time which make them less resistant to rutting.

The termination of FN is set to achieve any one of the two conditions, i.e., permanent strain of 5% or 10,000 loading cycles. Therefore, it requires more time to complete the test than the usual. The data obtained from the extensive lab testing were employed to develop a statistical model to predict pavement performance. This study used two different nonlinear formulations to predict axial strains from loading cycles. The general form of the model is given in the following equation:

$$\text{strain} = f(\text{load cycles}). \tag{3}$$

The data obtained from FN tests were subjected to initial scrutiny that suggests the power and polynomial (2nd order) formulation can best suit such a type of data. The generic form of these models is given in the following equation:

$$\begin{aligned} &(\text{power functional form}) Y = \alpha \times X_i^{\beta_i}, \\ &(\text{power functional form}) Y = \alpha + \beta \times X + \gamma \times X^2. \end{aligned} \tag{4}$$

This functional form can be rewritten for this study as follows:

$$\begin{aligned} \varepsilon_P &= \alpha \times N^{\beta}, \\ \varepsilon_P &= \alpha + \beta \times N + \beta \times N^2, \end{aligned} \tag{5}$$

where ε_P is the permanent strain, N is the loading cycles (10,000), and $\alpha, \beta,$ and γ are regression coefficients.

The model summary and statistics are presented in Table 3. t-Statistics of all variables are higher than t-critical ($|t^*| = 2.30$) at 95% confidence level, which implies that model variables are significant in predicting permanent strain. The coefficient of determination (R^2) is 0.99 and 0.91

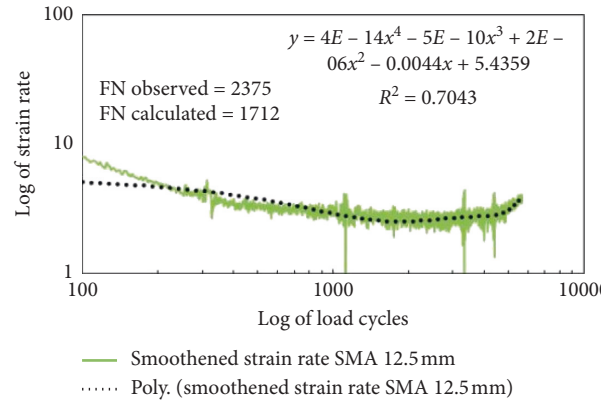

Figure 7: Data smoothening applied to 12.5 mm mix.

Table 2: FN test results.

Mixtures	FN value (seconds)	Accumulated strain@ FN (microstrains)	
	Corrected	AMPT	AMPT
25 mm	—	10000	11044
19 mm	—	10000	10194
12.5 mm	1712	2375	35819

for the power and polynomial model, respectively, which indicates that 99% and 91% of the variation in permanent strain is attributed to change in loading cycles.

The predictive capability of the developed model was assessed using mean absolute percentage error. It can be defined as the average of the absolute difference between the actual and predicted value:

$$\text{MAPE} = \frac{1}{n} \sum_{i=1}^{n} \left| \text{PE}_i \right|, \tag{6}$$

where $\text{PE}_i = 100 \times (X_i - P_i)/X_i$ is the percentage error for observation i of actual X_i and predicted P_i. X_i = actual/observed value. P_i = predicted value.

The MAPE value for the power and polynomial model is 0.19 and 0.20, respectively. A MAPE value of 0.19 (power model) represents on average, the predictions underestimate or overestimate the true values by 19%. The MAPE values closer to zero signify better accuracy.

The FT test was performed in accordance with NCHRP reports [35, 36] in which the preconditioned specimen is subjected to a constant axial load until it fails, and permanent deformation is measured with respect to the load time. The results indicate that, no any SMA mixture attained tertiary flow stage. Thus, no any data smoothening technique was required, and data acquired from AMPT software are used for comparison of accumulated strain at the time of termination of the test. The FT results suggest that all mixtures passed maximum cycles of 10,000, and mixtures are compared on the basis of accumulated strains. Table 4 indicates that, at time of termination, SMA 25 mm mix has a relatively small accumulated strain which suggests that this mix has relatively higher resistance to permanent deformation.

Table 3: Summary statistics of developed models.

Parameter	Estimate	Std. error	t-Statistics	N	R^2	95% CI	
						Lower	Upper
			Power Model				
α	19.956	0.155	128.75	200	0.99	19.653	20.26
β	0.69	0.001	690			0.689	0.692
			Polynomial Model				
α	−955.831	26.25	−36.41			−1007.3	−904.37
β	0.452	0.0002	2260	200	0.91	0.448	0.455
γ	125	2.787	44.85			119.155	130.083

Table 4: Accumulated strain values at termination.

Mixtures	Cycles (seconds)	Accumulated strain
SMA 25 mm	≥10000	5711
SMA 19 mm	≥10000	4868
SMA 12.5 mm	≥10000	9912

The results from this study—dynamic modulus, flow number, and flow time—would provide a foundation for evaluating pavement performance using M-EPDG. This design procedure entails both mechanistic and empirical procedure; dynamic modulus is used as a basic design input parameter at the first level of design in M-EPDG, which is mechanistic in nature. While for empirical evaluation, results from flow tests are used to develop flow models that predict pavement performance and serve as input to the second level of design in M-EPDG.

6. Summary and Conclusions

This paper presents the dynamic modulus testing of SMA mixtures at various temperatures (4.4–54.4°C) and frequencies (0.1–25 Hz) and flow number and flow time at a single effective temperature of 54°C. Given the tested SMA gradations/mixtures using limestone aggregate and 60/70 penetration grade, the dynamic modulus test reveals that, for a given loading frequency, an increase in temperature (from 21.1 to 37.8°C) translated into 41, 55, and 26% drop in $|E^*|$ values on average for 25 mm, 19 mm, and 12.5 mm mixtures, respectively. However, for a given temperature, an increase in loading frequency (from 0.1 to 25 Hz), 76, 85, and 74% of the variation in $|E^*|$ values on average was attributed for 25 mm, 19 mm, and 12.5 mm mixtures, respectively. Stress-dependent master curves were developed for each mix, and results indicated that 25 mm mix is relatively stiffer than other given mixtures. Resistance to fatigue cracking was evaluated using fatigue parameter, which shows that NMAS of 12.5 mm with a binder content of 5.3% has shown relatively better resistance to fatigue cracking. Statistical models were also developed to express permanent strain as a function of loading cycles. Also, flow test results showed that the SMA mixture with coarser gradation (NMAS 25 mm) having appropriate stone-to-stone contact exhibits excellent strength against rutting characteristics.

Data Availability

The gradation data, volumetric parameters, flow number, flow time test data, accumulated strain data, etc. used to support the findings of this study are included within the article. The master curve data, statistical parameter data, etc. used to support the findings of this study may be released upon application to Dr. Muhammad Irfan or Yasir Ali, who can be contacted via mirfan@mce.nust.edu.pk (Dr. Irfan) and yasirali@nit.nust.edu.pk (Yasir Ali).

Conflicts of Interest

The authors declare that they have no conflicts of interest.

Acknowledgments

The authors gratefully acknowledge the contribution of the National University of Sciences and Technology (NUST) laboratory support staff in preparing the samples for the research study.

References

[1] R. Bonaquist, D. Christensen, and W. Stump, "Simple performance tester for superpave mix design development and evaluations," NCHRP Report 513, Transportation Research Record, Washington, DC, USA, 2003.

[2] R. F. Bonaquist, *Refining the Simple Performance Tester for Use in Routine Practice*, Transportation Research Board, Washington, DC, USA, 2008.

[3] J. Judycki, "Influence of low-temperature physical hardening on stiffness and tensile strength of asphalt concrete and stone mastic asphalt," *Construction and Building Materials*, vol. 61, pp. 191–199, 2014.

[4] R. Muniandy, N. A. B. C. M. Akhir, S. Hassim, and D. Moazami, "Laboratory fatigue evaluation of modified and unmodified asphalt binders in stone mastic asphalt mixtures using a newly developed crack meander technique," *International Journal of Fatigue*, vol. 59, pp. 1–8, 2014.

[5] E. İskender, "Rutting evaluation of stone mastic asphalt for basalt and basalt–limestone aggregate combinations," *Composites Part B: Engineering*, vol. 54, pp. 255–264, 2013.

[6] T. B. Moghaddam, M. R. Karim, and T. Syammaun, "Dynamic properties of stone mastic asphalt mixtures containing waste plastic bottles," *Construction and Building Materials*, vol. 34, pp. 236–242, 2012.

[7] E. Ahmadinia, M. Zargar, M. R. Karim, M. Abdelaziz, and P. Shafigh, "Using waste plastic bottles as additive for stone

mastic asphalt," *Materials & Design*, vol. 32, no. 10, pp. 4844–4849, 2011.

[8] A. Behnood and M. Ameri, "Experimental investigation of stone matrix asphalt mixtures containing steel slag," *Scientia Iranica*, vol. 19, no. 5, pp. 1214–1219, 2012.

[9] C. E. Sengul, S. Oruc, E. Iskender, and A. Aksoy, "Evaluation of SBS modified stone mastic asphalt pavement performance," *Construction and Building Materials*, vol. 41, pp. 777–783, 2013.

[10] A. Khodaii, H. F. Haghshenas, H. Kazemi Tehrani, and M. Khedmati, "Application of response surface methodology to evaluate stone matrix asphalt stripping potential," *KSCE Journal of Civil Engineering*, vol. 17, no. 1, pp. 117–121, 2013.

[11] W. Cao, S. Liu, and Z. Feng, "Comparison of performance of stone matrix asphalt mixtures using basalt and limestone aggregates," *Construction and Building Materials*, vol. 41, pp. 474–479, 2013.

[12] M. Pasetto and N. Baldo, "Performance comparative analysis of stone mastic asphalts with electric arc furnace steel slag: a laboratory evaluation," *Materials and Structures*, vol. 45, no. 3, pp. 411–424, 2012.

[13] Å. L. Lyne, P. Redelius, M. Collin, and B. Birgisson, "Characterization of stripping properties of stone material in asphalt," *Materials and Structures*, vol. 46, no. 1-2, pp. 47–61, 2013.

[14] M. Irfan, M. Saeed, S. Ahmed, and Y. Ali, "Performance evaluation of elvaloy as a fuel-resistant polymer in asphaltic concrete airfield pavements," *Journal of Materials in Civil Engineering*, vol. 29, no. 10, article 04017163, 2017.

[15] J. Gao, H. Wang, Z. You, M. R. M. Hasan, Y. Lei, and M. Irfan, "Rheological behavior and sensitivity of wood-derived bio-oil modified asphalt binders," *Applied Sciences*, vol. 8, no. 6, p. 919, 2018.

[16] Y. Ali, M. Irfan, S. Ahmed, and S. Ahmed, "Permanent deformation prediction of asphalt concrete mixtures–a synthesis to explore a rational approach," *Construction and Building Materials*, vol. 153, pp. 588–597, 2017.

[17] Y. Ali, M. Irfan, S. Ahmed, and S. Ahmed, "Empirical correlation of permanent deformation tests for evaluating the rutting response of conventional asphaltic concrete mixtures," *Journal of Materials in Civil Engineering*, vol. 29, no. 8, article 04017059, 2017.

[18] Y. Ali, M. Irfan, S. Ahmed, S. Khanzada, and T. Mahmood, "Sensitivity analysis of dynamic response and fatigue behaviour of various asphalt concrete mixtures," *Fatigue & Fracture of Engineering Materials & Structures*, vol. 38, no. 10, pp. 1181–1193, 2015.

[19] Y. Ali, M. Irfan, S. Ahmed, S. Khanzada, and T. Mahmood, "Investigation of factors affecting dynamic modulus and phase angle of various asphalt concrete mixtures," *Materials and Structures*, vol. 49, no. 3, pp. 857–868, 2016.

[20] Y. Ali, M. Irfan, M. Zeeshan, I. Hafeez, and S. Ahmed, "Revisiting the relationship of dynamic and resilient modulus test for asphaltic concrete mixtures," *Construction and Building Materials*, vol. 170, pp. 698–707, 2018.

[21] M. Irfan, Y. Ali, S. Ahmed, and I. Hafeez, "Performance evaluation of crumb rubber-modified asphalt mixtures based on laboratory and field investigations," *Arabian Journal for Science and Engineering*, vol. 43, no. 4, pp. 1795–1806, 2018.

[22] M. Irfan, Y. Ali, S. Iqbal, S. Ahmed, and I. Hafeez, "Rutting evaluation of asphalt mixtures using static, dynamic, and repeated creep load tests," *Arabian Journal for Science and Engineering*, vol. 43, no. 10, pp. 5143–5155, 2018.

[23] M. Irfan, A. S. Waraich, S. Ahmed, and Y. Ali, "Characterization of various plant-produced asphalt concrete mixtures using dynamic modulus test," *Advances in Materials Science and Engineering*, vol. 2016, Article ID 5618427, 12 pages, 2016.

[24] M. Junaid, M. Irfan, S. Ahmed, and Y. Ali, "Effect of binder grade on performance parameters of asphaltic concrete paving mixtures," *International Journal of Pavement Research and Technology*, vol. 11, no. 5, pp. 435–444, 2018.

[25] I. Hafeez and M. A. Kamal, "Creep compliance: a parameter to predict rut performance of asphalt binders and mixtures," *Arabian Journal for Science and Engineering*, vol. 39, no. 8, pp. 5971–5978, 2014.

[26] Y. Kim, J. Lee, C. Baek, S. Yang, S. Kwon, and Y. Suh, "Performance evaluation of warm-and hot-mix asphalt mixtures based on laboratory and accelerated pavement tests," *Advances in Materials Science and Engineering*, vol. 2012, Article ID 901658, 9 pages, 2012.

[27] C. Kai, X. Wenyuan, C. Dan, and F. Huimin, "High-and low-temperature properties and thermal stability of silica fume/SBS composite-modified asphalt mortar," *Advances in Materials Science and Engineering*, vol. 2018, Article ID 1317436, 8 pages, 2018.

[28] M. A. Gul, M. Irfan, S. Ahmed, Y. Ali, and S. Khanzada, "Modelling and characterising the fatigue behaviour of asphaltic concrete mixtures," *Construction and Building Materials*, vol. 184, pp. 723–732, 2018.

[29] E. Brown and L. Cooley, "Designing of SMA for rut resistant pavements," NCHRP Report 425, National Cooperative Highway Research Program, Washington, DC, USA, 1999.

[30] E. R. Brown and J. E. Haddock, "Method to ensure stone-on-stone contact in stone matrix asphalt paving mixtures," *Transportation Research Record*, vol. 1583, no. 1, pp. 11–18, 1997.

[31] A. T. 62-07, *Standard Method of Test for Determining Dynamic Modulus of Hot-Mix Asphalt Concrete Mixture*, American Association of State Highway and Transportation Officials (AASHTO), Washington, DC, USA, 2006.

[32] M. Witczak, "Specification criteria for simple performance tests for rutting," NCHRP Report 580, National Cooperative Highway Research Program, Washington, DC, USA, 2007.

[33] Q. Ye, S. Wu, and N. Li, "Investigation of the dynamic and fatigue properties of fiber-modified asphalt mixtures," *International Journal of Fatigue*, vol. 31, no. 10, pp. 1598–1602, 2009.

[34] M. Witczak, K. Kaloush, T. Pellinen, M. El-Basyouny, and H. Von Quintus, "Simple performance test for superpave mix design," NCHRP Report 465, Transportation Research Board, Washington, DC, USA, 2002.

[35] R. F. Bonaquist, *Ruggedness Testing of the Dynamic Modulus and Flow Number Tests with the Simple Performance Tester*, NCHRP Report 629, Transportation Research Board, Washington, DC, USA, 2008

[36] M. Witczak, D. Andrei, and W. Houston, *Guide for Mechanistic–Empirical Design of New and Rehabilitated Pavement Structures*, Transportation Research Board of the National Research Council, Washington, DC, USA, 2004.